

Transition from collisional to kinetic regimes in large-scale reconnection layers

W. Daughton,¹ V. Roytershteyn,¹ B. J. Albright,¹ H. Karimabadi,² L. Yin,¹ and Kevin J. Bowers^{1,*}

¹*Los Alamos National Laboratory, Los Alamos, New Mexico 87544, USA*

²*University of California, San Diego, La Jolla, 92093*

(Received 10 February 2009; published 6 August 2009)

Using fully kinetic simulations with a Fokker-Planck collision operator, it is demonstrated that Sweet-Parker reconnection layers are unstable to plasmoids (secondary islands) for Lundquist numbers beyond $S \gtrsim 1000$. The instability is increasingly violent at higher Lundquist numbers, both in terms of the number of plasmoids produced and the super-Alfvénic growth rate. A dramatic enhancement in the reconnection rate is observed when the half-thickness of the current sheet between two plasmoids approaches the ion inertial length. During this transition to kinetic scales, the reconnection electric field rapidly exceeds the runaway limit, resulting in the formation of electron-scale current layers that are unstable to the continual formation of new plasmoids.

DOI: 10.1103/PhysRevLett.103.065004

PACS numbers: 52.35.Vd

The conversion of magnetic field energy into kinetic energy through the process of magnetic reconnection remains one of the most challenging and far-reaching problems in plasma physics. One key issue is the scaling of the reconnection dynamics for large-scale systems in nature. The magnetohydrodynamic (MHD) model is thought to provide an accurate description of *collisional* reconnection where the resistive layers are larger than the ion kinetic scale. For uniform resistivity, MHD gives rise to the celebrated Sweet-Parker (SP) model in which the reconnection rate scales as $U_{\text{in}}/V_A \approx \delta_{\text{sp}}/L_{\text{sp}} \approx S^{-1/2}$, where U_{in} is the inflow velocity, $V_A = B/\sqrt{4\pi m_i n}$ is Alfvén velocity, δ_{sp} is the half thickness and L_{sp} is the half length of the layer, $S = 4\pi V_A L_{\text{sp}}/\eta c^2$ is the Lundquist number, and η is the resistivity. Assuming that L_{sp} scales with the system size, implies $S \sim 10^6$ – 10^{14} for many applications. Since the resulting SP dissipation rates are much slower than observations, *collisional* is often used synonymously to denote *slow* reconnection [1].

Surprisingly, there is a fundamental flaw with these arguments that is not widely appreciated. The SP scaling is derived assuming the layers are structurally stable. However, for Lundquist numbers beyond $S \gtrsim 10^4$, MHD simulations indicate that laminar SP layers are unstable to plasmoid formation [2], while plasmoids are observed at even lower S when turbulence is imposed [3]. Furthermore, linear theory [4] predicts a growth rate that scales as $S^{1/4} V_A/L_{\text{sp}}$ with the number of plasmoids increasing with $S^{3/8}$. Thus the scaling of *collisional* reconnection remains uncertain in the high S regime.

One important consequence of plasmoid formation is that it may potentially lead to the breakdown of MHD. To illustrate this point, assume that N_p plasmoids form within the original SP layer and that the new layers between the islands also follow the same SP scaling but with a reduced layer length $\sim L_{\text{sp}}/N_p$. This implies the thickness δ of the new layers scales as $\delta/\delta_{\text{sp}} \sim 1/\sqrt{N_p}$, where δ_{sp} is the half-

thickness of the original SP layer. When $N_p \gg 1$, it is possible for δ to reach the ion kinetic scale much sooner than would be expected for the original SP layer. Reconnection physics changes drastically when resistive layers approach the ion kinetic scale. In neutral sheet geometry, both two-fluid simulations [5,6] and theory [7] predict a transition when $\delta_{\text{sp}} \leq d_i$ where d_i is the ion inertial length. This regime is often referred to as *kinetic* or *fast* reconnection since a variety of two-fluid and kinetic models predict rates that are weakly dependent on the system size and dissipation [8], although the precise scalings are still controversial [9].

The transition between collisional and kinetic regimes was recently proposed as a mechanism for regulating coronal heating [1]. However, these estimates were based on the assumption of a stable SP layer. In order to address the influence of plasmoids, this work employs fully kinetic simulations with a Monte Carlo treatment of the Fokker-Planck collision operator [10]. In regimes where SP layers are stable $S \lesssim 1000$, this first-principles approach has demonstrated a clear transition to the kinetic regime near the expected threshold $\delta_{\text{sp}} \approx d_i$ [11]. Here we demonstrate that SP layers are increasingly unstable to plasmoid formation in large-scale systems. Since the observed growth is faster than L_{sp}/V_A , this super-Alfvénic instability allows the islands to reach large amplitude before they are convected downstream. A dramatic enhancement in the reconnection rate is observed when the current sheet between two plasmoids approaches the ion inertial scale. During this transition, the reconnection electric field exceeds the runaway limit leading to a collapse of the diffusion region current sheet to the electron kinetic scale. These electron layers form elongated current sheets which are also unstable to the formation of new plasmoids in a manner similar to the collisionless limit [12]. Certain aspects of this complex evolution are similar to the phenomenological model in Ref. [13].

The simulations were performed with the VPIC [14] code which has been modified to include Coulomb collisions and benchmarked against transport theory [11]. The initial condition is a Harris sheet with magnetic field $B_x = B_o \tanh(z/\lambda)$ and density $n = n_o \text{sech}^2(z/\lambda)$ provided by drifting Maxwellian distributions with uniform temperature $T_e = T_i = T_o$ ($\lambda = 2d_i$ is the half-thickness of the current sheet). A uniform nondrifting background is included with density $n_b = 0.3n_o$ and equal temperature. Other parameters are $m_i/m_e = 40$, $\omega_{pe}/\Omega_{eo} = 2$, where $\omega_{pe} = \sqrt{4\pi n_o e^2}/m_e$ is the electron plasma frequency, $v_{\text{the}}/c = 0.35$ where $v_{\text{the}} = (2T_o/m_e)^{1/2}$ is the electron thermal speed. Lengths are normalized to the ion inertial length $d_i = c/\omega_{pi}$ where $\omega_{pi} = \sqrt{4\pi n_o e^2}/m_i$ and time is normalized to $\Omega_{io} = eB_o/(m_i c)$. The local ion d_{i*} and electron d_{e*} inertial lengths are based on the time evolving central layer density.

A Fokker-Planck treatment of Coulomb collisions gives rise to a number of complications not normally considered in fluid calculations [11]. In neutral sheet geometry, the resistivity perpendicular to the magnetic field η_{\perp} plays the dominant role in setting the structure of the SP layer, except for a small region near the x point where the local electron cyclotron frequency falls below the electron-ion collision frequency ($\Omega_e < \nu_{ei}$). Furthermore, the resistivity varies in both space and time due to electron Ohmic heating within the layer

$$\hat{\eta}_{\perp} \equiv \frac{\omega_{pi}^2}{4\pi\Omega_{io}} \eta_{\perp} = \hat{\eta}_{\perp o} \left(\frac{T_o}{T_e}\right)^{3/2}, \quad (1)$$

where T_e the local electron temperature and $\hat{\eta}_{\perp o} = 0.04$ is the initial resistivity for all simulations in this study. The coefficient $\hat{\eta}_{\perp o}$ is set by scaling ν_{ei} and the subsequent time evolution of $\hat{\eta}_{\perp}$ is well described [11] by (1) for parameter regimes in which the reconnection electric field E_y is small in comparison to the runaway limit $E_{\text{cr}} \approx (m_e T_e/2)^{1/2} \nu_{ei}/e$. Within the collisional SP regime, this ratio is approximately $E_y/E_{\text{cr}} \sim (d_i/\delta_{\text{sp}})(m_e/m_i)^{1/2}$, which implies that SP layers are always in a regime where (1) is valid. During the transition to the kinetic regime, the rapid increase in the reconnection rate can lead to runaway fields $E_y > E_{\text{cr}}$ where (1) breaks down.

The simulation parameters are summarized in Table I, along with the initial Lundquist number S_o computed using $\hat{\eta}_{\perp o} = 0.04$ and the maximum Lundquist number S_{max} computed using $\hat{\eta}_{\perp}$ in the layer at the time of the transition. The time step for all simulations was $\Delta t \Omega_{ce} = 0.13$ with 1000 particles per cell for each species. The boundary conditions are periodic in the x direction for both particles and fields while the z boundaries are conducting for fields and reflecting for particles.

For periodic boundary conditions, simulations [6,11] indicate the half-length of the SP layer is approximately $L_{\text{sp}} \approx L_x/4$ where L_x is the system size in the x direction. Assuming the SP layer is stable, the two-fluid transition

TABLE I. Summary of parameters: System size L_x , cells N_x , Lundquist number $S_o \equiv 4\pi V_A L_{\text{sp}}/(\eta_{\perp o} c^2)$ based on the initial resistivity $\hat{\eta}_{\perp o} = 0.04$ and assuming $L_{\text{sp}} \approx L_x/4$, maximum Lundquist number $S_{\text{max}} \equiv 4\pi V_A L_{\text{sp}}/(\eta_{\perp} c^2)$ due to electron heating in the layer, predicted transition resistivity $\hat{\eta}_c$ required for $\delta_{\text{sp}} \approx d_i$, the actual resistivity $\hat{\eta}_{\perp}$ within the layer at the transition time τ , the number of plasmoids N_p within the SP layer and the transition time τ normalized to the Alfvén time $\tau_A = L_{\text{sp}}/V_A$. The transverse size is $L_z = 100d_i$ with 1600 cells for all cases.

L_x/d_i	N_x	S_o	S_{max}	$\hat{\eta}_c$	$\hat{\eta}_{\perp}$	N_p	τ/τ_A
100	1600	625	1140	0.04	0.025	0	...
200	3200	1250	2500	0.02	0.020	3	2.7
400	6400	2500	5000	0.01	0.019	4	1.8
800	12 800	5000	11 700	0.005	0.018	7	1.2

condition $\delta_{\text{sp}} \leq d_i$ may be reexpressed as

$$\hat{\eta}_{\perp} \leq \frac{d_i}{L_{\text{sp}}} \approx \frac{4d_i}{L_x} \equiv \hat{\eta}_c, \quad (2)$$

where $\hat{\eta}_c$ is the critical transition resistivity. For the smallest simulation in Table I, this is equal to the initial resistivity while the larger simulations require increasing amounts of Ohmic heating in order to reduce the resistivity in the layer to this critical value.

The simulations are initiated with a small magnetic perturbation using the same functional form as Ref. [11] with magnitude $\delta B_z = 0.025B_o$. The reconnection rate is calculated from $E_R = \langle \partial \psi / \partial t \rangle / (BV_A)$, where $\psi = \max(A_y) - \min(A_y)$ along $z = 0$, A_y is the y component of the vector potential, B and V_A are evaluated at $10d_i$ upstream of the dominant x point and $\langle \rangle$ represents a time average over $\Delta t \Omega_{io} = \pm 5$ to reduce noise.

The resulting reconnection rates are shown in the left panel of Fig. 1 for the time interval $t \Omega_{io} = 0 \rightarrow 100$. As expected for the SP regime, the rates are progressively slower for the larger systems. Since the initial resistivity and sheet thickness are the same for all simulations, the evolution of the electron temperature and resistivity are also quite similar. Thus the SP scaling prediction can be tested by plotting the average rate as function of $(d_i/L_x)^{1/2}$ as illustrated in the right panel. These results demonstrate

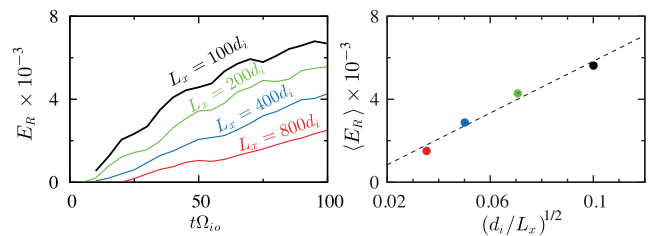


FIG. 1 (color). Evolution of the reconnection rates (left) at early time and the average reconnection rate (right) over the interval $t \Omega_{io} = 40 \rightarrow 100$ as a function of $(d_i/L_x)^{1/2}$. The dashed line is the best-fit linear regression.

that the kinetic simulations have recovered the SP scaling during this time interval.

Over longer time scales, all simulations in Table I transition to much faster reconnection rates. The smallest $L_x = 100d_i$ simulation remains in a stable SP configuration until the half-thickness of the layer reaches d_i . In this case, the transition to the kinetic regime is very similar to the results described in Ref. [11]. Because of limited space, the rest of this Letter is focused on the three largest cases in Table I. As illustrated in the top panel of Fig. 2, the reconnection rates increase dramatically near the transition times highlighted by the vertical dashed lines. In contrast to the early time evolution in Fig. 1, the average rates at late time actually *increase* slightly for the larger systems. To examine condition (2), the second panel shows the evolution of the resistivity $\hat{\eta}_\perp$ normalized to the critical value $\hat{\eta}_c$ for each case. While the $L_x = 200$ case transitions near the expected threshold (2), the larger simulations transition at

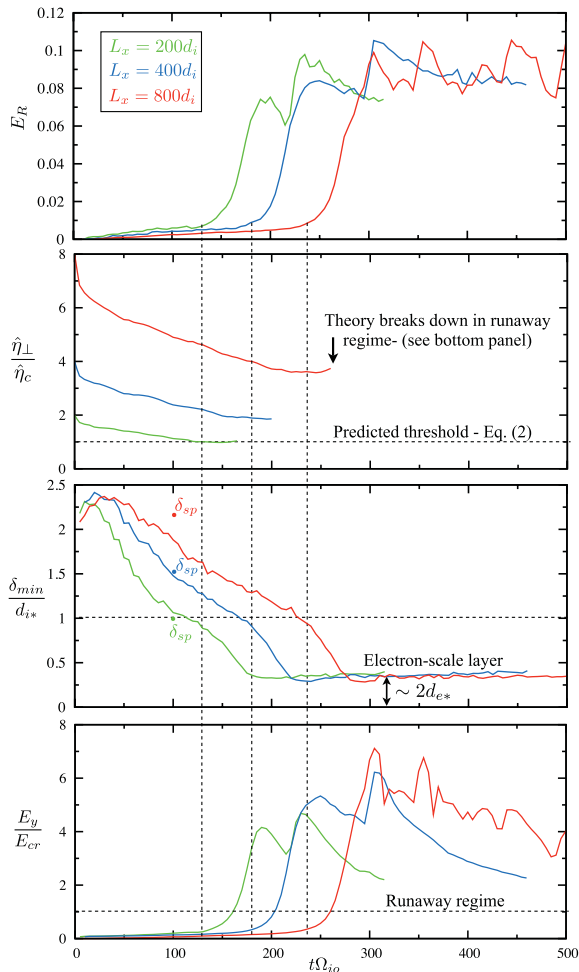


FIG. 2 (color). Evolution of the rate E_R , the resistivity $\hat{\eta}_\perp$ implied by (1) normalized to $\hat{\eta}_c$ from (2), the minimum layer thickness δ_{\min} and the electric field E_y normalized by the runaway field E_{cr} . The transition time τ is highlighted by a vertical line for each case. The circles in the third panel correspond to the theoretical estimate for δ_{sp} at time $t\Omega_{io} \approx 100$ (see text).

increasingly higher resistivities due to the formation of plasmoids. As summarized in Table I, the number of plasmoids in the SP layer near the transition time increases significantly for higher S , with a chain of ~ 7 plasmoids for the largest case.

To better illustrate the structural evolution, the current density J_y and flux surfaces are given in Fig. 3 for the $L_x = 800d_i$ case. During the initial evolution $t\Omega_{io} \lesssim 200$, the reconnection layer resembles the classic SP configuration as shown in the top panel. However, closer inspection reveals the initial growth of the instability at $t\Omega_{io} \sim 140$, and a chain of plasmoids is clearly visible at $t\Omega_{io} = 250$ in the second panel. These plasmoids break the SP layer into a series of separate reconnection sites with a current sheet

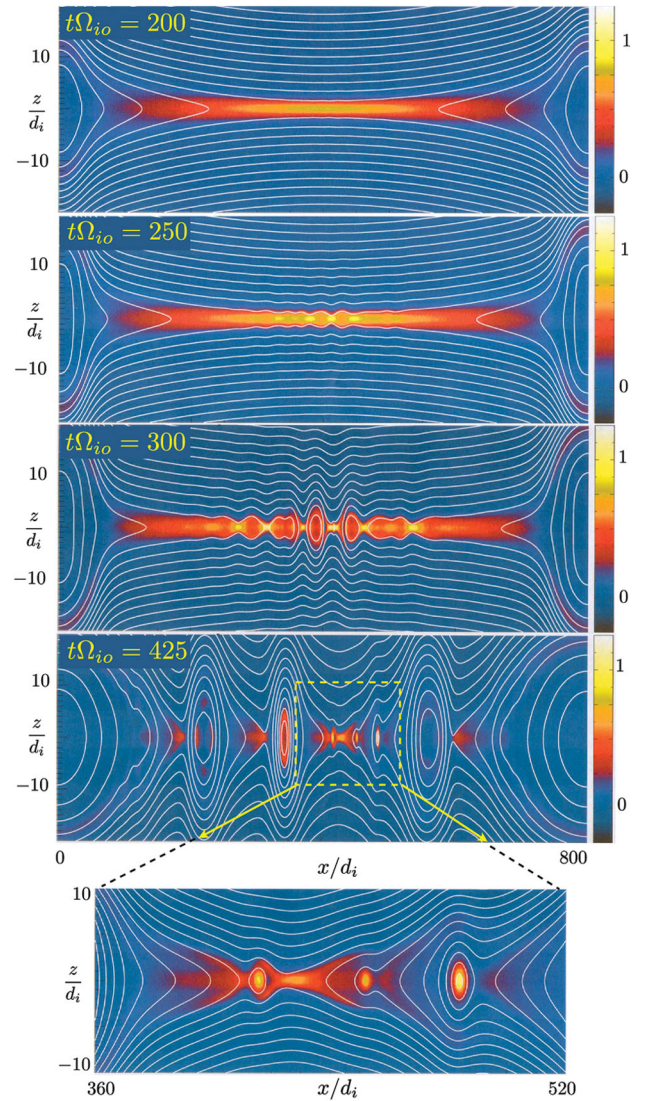


FIG. 3 (color). Time evolution of the current density J_y for the largest $L_x = 800d_i$ simulation. White lines are the magnetic flux surfaces and the bottom panel is a close-up of the region indicated at $t\Omega_{io} = 425$ to illustrate the repeated formation of new plasmoids within the electron layer. The current density is normalized to the initial peak value $J_o = cB_o/(4\pi\lambda)$.

between each island as illustrated in the third panel at $t\Omega_{io} = 300$.

In order to measure the scale of the various current layers during this complex evolution, a diagnostic was constructed to scan across the system in the x direction and measured the half thickness of the current profile at each location. The minimum half thickness δ_{\min} resulting from this procedure is shown in the third panel of Fig. 2. Within the initial SP regime, δ_{\min} is in reasonable agreement with the theoretical SP thickness as indicated by the respective circles at $t\Omega_{io} \approx 100$ computed using $\delta_{\text{sp}}/d_i \approx (L_{\text{sp}} \hat{\eta}_{\perp}/d_i)^{1/2}$. While the $L_x = 200d_i$ simulation is already near $\delta_{\min} \approx d_i$, the other two simulations would not be expected to transition based on the observed electron heating (and reduction of resistivity). However, the growth of plasmoids leads to the intensification of the current density between the islands, and there is a dramatic increase in the reconnection rate when the thickness of these layers approach $\delta_{\min} \approx d_{i*}$.

This transition criterion is consistent with the increasing importance of Hall physics for layers of this scale [5,6]. However, the significant differences with two-fluid models in the subsequent evolution indicate that nonideal electron physics is also playing a crucial role in the kinetic regime. In particular, the reconnection electric field greatly exceeds the runaway limit as illustrated in the bottom panel of Fig. 2. As a consequence, the diffusion region current layer collapses to the electron scale $\delta_{\min} \approx 2d_{e*}$. In this runaway regime, collisional momentum exchange is increasingly ineffective and the reconnection electric field is balanced predominantly by the divergence of the electron pressure tensor [11]. The electron layers form elongated sheets which are unstable to the repeated formation of new plasmoids (see bottom panel of Fig. 3). In this example, 6 new plasmoids are generated within the central electron layer leading to significant time modulations in the rate similar to recent collisionless kinetic simulations [12].

These first-principles kinetic simulations indicate that the instability of Sweet-Parker layers at high S can play a crucial role in determining the transition to kinetic regimes. Although it is difficult to infer reliable scalings from this limited study, the number of plasmoids in Table I increases roughly as $N_p \propto S^{0.6}$ while the onset time decreases $\tau/\tau_A \propto S^{-0.5}$. These scalings are in the same direction as MHD theory [4], but are somewhat stronger functions of S . These trends imply an increasingly violent instability at large S , with super-Alfvénic growth rates that permit the plasmoids to reach large amplitude before they are convected downstream. The new current layers between plasmoids are significantly thinner than the original SP layer which leads to a rapid increase in the rate when these layers approach the ion inertial scale.

These results may have profound implications for reconnection in the solar corona. Previous estimates for the transition to the kinetic regime [1] are only valid for low S where SP layers are stable. These estimates imply the

transition resistivity (2) is strongly dependent on the system size, while the influence of plasmoids in the present study gives rise to a very weak dependence. In future work, it may be possible to construct new transition estimates based on firm knowledge of two key ingredients: (i) the scaling for the number of plasmoids $N_p \propto S^{\alpha}$ and (ii) the thickness δ of the new layers. For example, assuming δ obeys the SP scaling, the transition to the kinetic regime $\delta \approx d_i$ corresponds to $\hat{\eta}_c \propto (d_i/L_x)^{\gamma}$ where $\gamma = (1 - \alpha)/(1 + \alpha)$. Using the estimate of $\alpha \approx 0.6$ implies $\gamma \approx 0.25$ which is still somewhat stronger than the observed trend in Table I. While there are significant uncertainties with both of these assumptions, this basic trend implies that reconnection may proceed much more readily than previous estimates which neglected plasmoids. This could potentially raise new questions regarding how magnetic energy builds up in active regions.

We acknowledge support from the U.S. DOE through the LANL-LDRD Program. Contributions from H. K. were supported by the NASA Heliophysics Theory Program and NSF GEM grant ATM 0802380.

*Guest Scientist. Currently with D. E. Shaw Research, LLC, New York, NY 10036, USA.

- [1] P. Cassak, J. Drake, and M. Shay, *Astrophys. J.* **644**, L145 (2006); D. Uzdensky, *Astrophys. J.* **671**, 2139 (2007), and references therein.
- [2] D. Biskamp, *Phys. Fluids* **29**, 1520 (1986); M. Yan, L. Lee, and E. Priest, *J. Geophys. Res.* **97**, 8277 (1992); G. Lapenta, *Phys. Rev. Lett.* **100**, 235001 (2008); A. Bhattacharjee, Yi-Min Huang, H. Yang, and B. Rogers, "Fast Reconnection in High-Lundquist Number Plasmas due to Secondary Tearing Instabilities" *Phys. Plasmas* (to be published).
- [3] W. Matthaeus and S. Lamkin, *Phys. Fluids* **28**, 303 (1985).
- [4] N.F. Loureiro, A.A. Schekochihin, and S.C. Cowley, *Phys. Plasmas* **14**, 100703 (2007).
- [5] Z. Ma and A. Bhattacharjee, *Geophys. Res. Lett.* **23**, 1673 (1996).
- [6] P. Cassak, M. Shay, and J. Drake, *Phys. Rev. Lett.* **95**, 235002 (2005).
- [7] A.N. Simakov and L. Chacón, *Phys. Rev. Lett.* **101**, 105003 (2008).
- [8] J. Birn, J. Drake, and M. Shay *et al.*, *J. Geophys. Res.* **106**, 3715 (2001); M. Shay, J. Drake, and B. Rogers *et al.*, *J. Geophys. Res.* **106**, 3759 (2001).
- [9] A. Bhattacharjee, K. Germaschewski, and C. Ng, *Phys. Plasmas* **12**, 042305 (2005).
- [10] T. Takizuka and H. Abe, *J. Comput. Phys.* **25**, 205 (1977).
- [11] W. Daughton, V. Roytershteyn, and B. Albright *et al.*, *Phys. Plasmas* **16**, 072117 (2009).
- [12] W. Daughton, J. Scudder, and H. Karimabadi, *Phys. Plasmas* **13**, 072101 (2006); A. Klimas, M. Hesse, and S. Zenitani, *Phys. Plasmas* **15**, 082102 (2008).
- [13] K. Shibata and S. Tanuma, *Earth Planets Space* **53**, 473 (2001).
- [14] K.J. Bowers, B.J. Albright, and L. Yin *et al.*, *Phys. Plasmas* **15**, 055703 (2008).